J Solid State Electrochem
DOI 10.1007/s10008-016-3312-6

ORIGINAL PAPER

Electrochemistry of Tris(1,10-phenanthroline)iron(II) inside a polymeric hydrogel. Coupled chemical reactions and migration effects

Maria Victoria Martinez[1] · Rusbel Coneo Rodriguez[1] · Angelica Baena Moncada[1] · Claudia R. Rivarola[1] · Mariano M. Bruno[1] · Maria C. Miras[1] · Cesar A. Barbero[1]

Received: 24 March 2016 / Revised: 18 June 2016 / Accepted: 28 June 2016

Abstract The retention, release, and detection of metallic complexes in polymeric hydrogels are of interest in drug delivery, analytical chemistry, and water remediation. The electrochemistry of the redox complexes inside the hydrogel could be affected by the viscoelastic properties of the gel, local ionic force and pH, and interactions (e.g., hydrophobic) between the complex and the polymer chains. In this work, it is shown that a simple setup, consisting of a disk electrode pressed on the hydrogel, allows to perform electrochemistry of a redox couple: Tris(1,10-phenanthroline)iron(II) ($Fe(phen)_3^{2+}$) inside a hydrogel matrix. The behavior is compared with the same couple in solution, and it is found that the electrochemical properties of the redox couple are strongly affected by the presence of the hydrogel matrix. The cyclic voltammogram of the hydrogel loaded with complex shows a response, which suggests electrochemical-chemical mechanism. The chemical step is likely linked to a catalytic oxidation of free hydrated Fe^{2+} ions present inside the hydrogel together with the redox complex. Since Fe^{2+} ions have small charge transfer constants on the glassy carbon electrodes, only the catalytic current is observed. Indeed, when excess ligand (phenanthroline) is absorbed inside the hydrogel, the measured cyclic voltammograms show a single reversible oxidation/reduction step. It seems that the complexation equilibrium shifts toward the complex, making the free iron concentration negligible. Accordingly, the cyclic voltammetry shape and peak potential difference agree with a reversible oxidation/reduction. Additionally, the peak currents of the cyclic voltammograms show a linear dependence with the square root of time, as predicted by a Randles-Sevcik equation. However, the measured currents are smaller than the simulated ones. The differences are in agreement with simulations of the cyclic voltammograms where the migration of the redox species is considered. Chronoamperometry is used to measure the mass transport of redox species inside the hydrogel. It is found that the current transients still obey Cottrell's equation, but the diffusion coefficients obtained from the slopes of Cottrell's plots have to be corrected for migration effects. The effective diffusion coefficient of $Fe(phen)_3^{2+}$ measured inside the hydrogel ($D_{\text{Red-hydrogel}}$ = 5.5 (±0.5) × 10^{-8} cm^2 s^{-1}) is ca. 80 times smaller than the one measured in solution ($D_{\text{Red-solution}}$ = 4.4 (±0.5) × 10^{-6} cm^2 s^{-1}). The simple setup has a true semi-infinite boundary condition, which allows characterizing the hydrogel in the same condition as the bulk material and easily changing both the redox species and the hydrogel structure.

Keywords Hydrogel · Phenanthroline · Iron · Partition

Introduction

Polymeric hydrogels are crosslinked polymer networks where the linear chains, between crosslinks, are hydrophilic and retain a significant amount (>80 %) of aqueous solution, even as free-standing solids [1]. Such materials have been used for different technological applications, including contact lenses, diapers, drug delivery, and water retention in agriculture [2]. The hydrogels are also routinely used in biochemical research as solid media for electrophoretic separations [3]. It is known that the gels absorb specific molecules or ions and it is possible to define a partition coefficient (*Cp*) of the chemical

Electronic supplementary material The online version of this article (doi:10.1007/s10008-016-3312-6) contains supplementary material, which is available to authorized users.

✉ Cesar A. Barbero
cbarbero@exa.unrc.edu.ar

[1] Chemistry Department, Universidad Nacional de Rio Cuarto - CONICET, 5800 Rio Cuarto, Argentina

Published online: 16 July 2016

species between the surrounding solution and the hydrogel phase [4]. Large values of *Cp* (>100) have been usually measured, suggesting that chemical species are specifically retained inside the solid gel [4]. The partition depends on different interactions of the chemical species with the polymer matrix, including Coulombic, hydrophobic, hydrogen bonding, etc. Such specific absorption of chemical species inside the gel could be used for solid phase extraction of analytes from aqueous solutions [5, 6]. Since the gel phase can be mechanically separated from the aqueous solution, it is analog to a liquid-liquid extraction [7]. In liquid-liquid extraction of ions, the usual strategy is to dissolve a complexing agent in the organic phase, which extracts the ion from the aqueous solution by complexation. We have shown that some complexes, like $Ru(bpy)_3^{2+}$, show large partition coefficients toward polyacrylamides [4]. If a complexing agent (e.g., phenanthroline) is retained inside a hydrogel by hydrophobic and/or Coulombic interactions, it will concentrate inside the hydrogel a specific ion (e.g. Fe^{2+}) from water solution through the formation of a complex.

The electrochemistry of electroactive polymers, where the redox groups are covalently linked to the polymer chains [8–13], including some containing the phenanthroline group [14, 15] has been thoroughly studied. Additionally, the immobilized redox complexes have been used to catalyze redox reactions, which have slow charge transfer in common electrodes, through an electrochemical chemical(catalytic) mechanism [16]. However, the synthesis of polymers bearing redox groups or linking points is complex. The changes in the chemical structure (e.g., by copolymerization) affect not only the polymeric environment of the redox couples but also its intrinsic properties. One way to separate the effects is to study the electrochemistry of ion complexes loaded inside polyelectrolyte films [17–21]. However, the diversity of chemical structures of the polymer matrixes already studied has been quite limited. Moreover, the deposition of thin films on the electrode could produce a material which is not the same as the bulk material. The most common deposition procedure, which is solution casting, could not be applied to bulk crosslinked hydrogels.

Tris(1,10-phenanthroline)iron(II) complex ($Fe(phen)_3^{2+}$) is a redox active complex, which is both used for colorimetric detection of iron and as redox indicator [22]. The electrochemistry of iron phenanthroline has been previously studied in solution [23, 24]. Moreover, it was used as redox probe to detect interactions with DNA [25]. Hydrogels bearing phenanthroline moieties linked to the polymer chains have been synthesized and used in the colorimetric determination of iron [26]. In the best of our knowledge, the electrochemistry of Tris(1,10-phenanthroline)iron(II) complex inside covalently linked hydrogels has not been studied previously.

In the present work, we have used a simple electrochemical setup to study the electrochemistry of $Fe(phen)_3^{2+}$ loaded inside a polymeric crosslinked hydrogel (poly(acrylamide-co-acrylamido-2-methylpropanesulfonic acid)). The results are compared with those obtained in solution. Strong effects of the hydrogel matrix on the electrochemical responses are observed. The observed electrochemical-chemical mechanism, likely due to the redox catalysis of free iron, is studied using digital simulation of the cyclic voltammetric response. Loading excess ligand inside the hydrogel, the free iron concentration is reduced and the voltammetric response obeys a mechanism of a single reversible electron step. The mass transport parameters (diffusion coefficients) are measured using chronoamperometry. Both the cyclic voltammetry and the chronoamperometric transients reveal the existence of migration effects, which are taken into account.

Experimental

All chemicals are of analytical quality. Millipore (1.8 Mohm) purified water was used to prepare the solutions.

Materials and methods

Synthesis of hydrogel matrix

Poly(acrylamide-co-acrylamido-2-methylpropanesulfonic acid) (P(AAm-co-AMPS) hydrogel was synthesized via free-radical copolymerization of acrylamide (AAm) (Fluka) (1 M) with 2-acrylamido-2-methylpropanesulfonic acid (AMPS) (Scientific Polymer Products) (1 M) (Scheme 1). *N*,*N*′-methylenebisacrylamide (BIS) (Aldrich) was used as cross-linker agent. The radical polymerization was initiated thermally by 2,2′-azobis(2-methylpropionamidine) dihydrochloride (V50) (Aldrich). This is decomposed at temperature higher than 56 °C to generate free radicals. In this synthesis, a buffer solution pH = 10 was used as solvent. The monomers and cross-linker (BIS, 2 % moles based on copolymer) were placed in a tube and the buffer was added until a final volume of 4 mL; then, the solution was purged by bubbling with N_2 gas and the initiator (V50 (0.003 g/mL)) is added. The polymerization was carried out in a sealed glass tube in a water bath at 60 °C to allow the initiator decomposition. The tube was left in the bath until gelation (ca. 15 min). When the polymerization was completed, the hydrogels were immersed in distilled water at room temperature for 48 h and the water was renewed several times in order to remove unreacted chemicals. The hydrogels swell significantly in water, with a volume increase of ca. 121 times of the dry hydrogel.

Scheme 1 Chemical structure of the monomers in the polymerization of P(AAm-co-AMPS) hydrogel

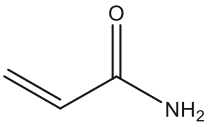

Acrylamide (**AAm**)

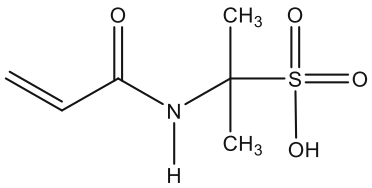

2-acrylamido-2-methylpropanesulfonic acid (**AMPS**)

Phenanthroline loading process into PAAm-co-50 % AMPS and absorption of Fe^{2+}

The dry hydrogel was swollen in 1×10^{-3}-M phenanthroline solution for 48 h and then dried in a stove at 40 °C to remove the solvent. The dry gel loaded with the molecule was then swollen in $[Fe^{2+}] = 1 \times 10^{-3}$-M solution (made from hydrated ferrous sulfate $(SO_4Fe)(H_2O)_7$) (Mallinckrodt), with traces of hydrazine to avoid the Fe^{2+} to Fe^{3+} oxidation), during 48 h.

Partition coefficient

Equation 1 describes the calculation of partition coefficient from the complex molar concentration inside the hydrogel ($[Fe(phen)_3{}^{2+}]_{hydrogel}$) and the complex molar concentration in solution (after reaching equilibrium) ($[Fe(phen)_3{}^{2+}]$solution). The latter is measured using UV-vis spectrophotometry, and the former is calculated by difference

$$Cp_{\text{molar}} = \frac{\left[\text{Fe(Phen)}_3^{2+}\right]_{\text{hydrogel}}}{\left[\text{Fe(Phen)}_3^{2+}\right]_{\text{solution}}} \quad (1)$$

The measured Cp_{molar} for $[Fe(phen)_3{}^{2+}]$ in PAAm-co-50 % AMPS is 57 (±) 0.5.

Electrochemistry

A 3-mm glassy carbon disk, inserted in a Kel-F shroud and contacted in the back with silver paste, was used as working electrode. The reference was a silver wire (0.5 mm) where a thick layer of AgCl was deposited by anodic oxidation in 1-M KCl solution. The wire is placed inside a Luggin capillary filled with 1-M KCl solution. A Pt wire was used as counterelectrode. The electrochemical experiments were controlled by a computer-controlled potentiostat (Autolab PGSTAT30, Ecochemie). Cyclic voltammetry experiments were carried between 0.7 and 1.2 V at 5 mV s^{-1}: first with the electrode exposed to the solution and then with the electrode gently pressed onto the hydrogel. No effect of pressure was observed, once a clear mechanical contact between the electrode and the hydrogel is observed. In analog fashion, chronoamperometric experiments were carried out stepping the potential between 0.7 and 1.2 V, after a 2-min preconditioning at 0.7 V. In Scheme 2, it is described the electrochemical cell used. The solution of the cell is 1 M KCl, and the pH is measured to be 6 for all experiments. All potentials are reported against the standard hydrogen electrode (NHE).

Digital simulation

Digital simulation of cyclic voltammetric experiments was performed using the Electrochemical Simulation Package (ESP 2.1), a program written by Carlo Nervi [27]. The simulations were performed in a personal computer (Pentium III, 1-Gb RAM, 40-Gb hard disk) running DOS (inside a Windows XP environment). The simulated data points were then imported into Origin 7.0 (Microcal) for comparison with experimental data.

Results and discussion

Cyclic voltammetry of $Fe(phen)_3{}^{2+}$ in solution and inside the hydrogel

In Fig. 1, it is shown the electrochemical response of $Fe(phen)_3{}^{2+}$ in both media. The cyclic voltammogram measured in solution (Fig. 1a) shows a profile in agreement with a single reversible oxidation/reduction step

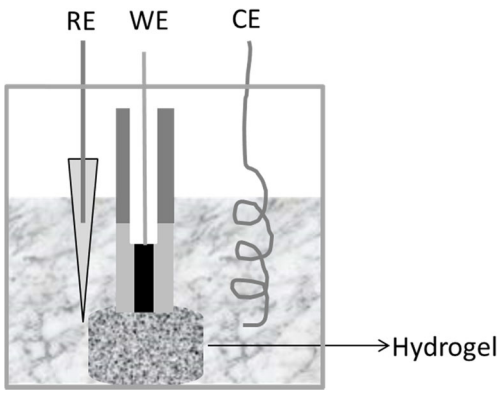

Scheme 2 Setup for electrochemical measurement. *WE* working electrode (glassy carbon disk (3-mm dia.), *RE* reference electrode (Ag/AgCl), *CE* counterelectrode (platinum wire)

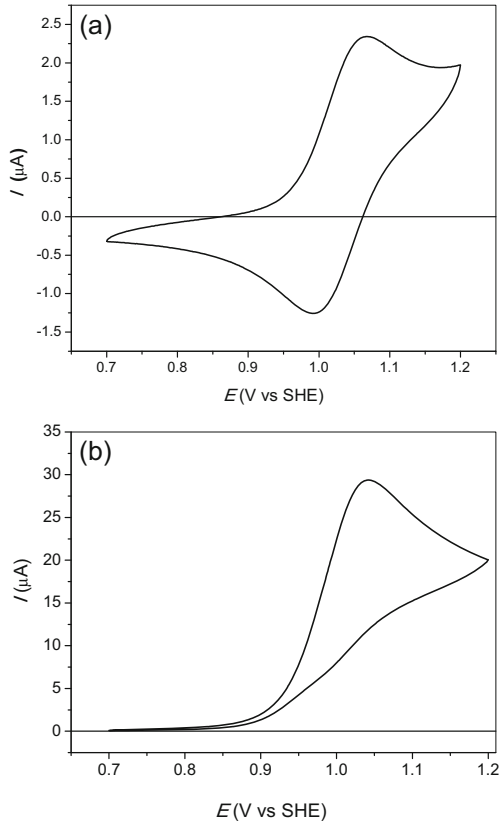

Fig. 1 Cyclic voltammograms of a glassy carbon electrode in **a** 0.2 mM $[Fe(phen)_3]^{2+}$ in 1 M KCl and **b** 11.4 mM $[Fe(phen)_3]^{2+}$ loaded in a poly(AAm-co-AMPS) hydrogel. $A = 0.071\ cm^2$, $v = 5\ mV\ s^{-1}$. $T = 25\ °C$. The second cycle is shown in both cases

(ΔEp = 0.059 mV) in the potential range studied. The data agree with previous results [23–25].

On the other hand, the cyclic voltammogram of $Fe(phen)_3^{2+}$ loaded inside the gel shows a quite different profile (Fig. 1b). The cyclic voltammogram shows positive current values during the forward scan and small current values during the backward scan. This shape is compatible with an electrochemical-chemical mechanism. The details of mechanism will be ascertained below using digital simulation. It can be seen that the anodic peak current for the cyclic voltammogram measured inside the hydrogel (ca. 29.3 μA) is significantly larger than the peak current measured in solution (2.36 μA). The increased sensitivity (ca. 12 times) upon the same conditions is important for the use of the system in the electroanalytical determination of iron. However, if the peak current would be directly proportional to concentration, the signal should have increase 57 times (equal to the partition coefficient). Obviously, the current signal decreases due to changes in the mass transport and/or reaction mechanism due to the presence of the hydrogel matrix.

However, it is clear that the simple setup allows measuring the electrochemistry of the redox couple inside the hydrogel. To separate the effects of mass transport and reaction mechanism, different electrochemical methods are used.

Chronoamperometry of redox species in solution and inside the hydrogel

To quantify the change in mass transport, chronoamperometric measurements were performed. The potential is stepped from a potential (0.7 V) where no reaction occurs to a positive-enough potential (1.2 V), where all the $Fe(phen)_3^{2+}$ is oxidized at the electrode/electrolyte (solution or hydrogel) interface. In Fig. 2, the chronoamperometric response of $Fe(phen)_3^{2+}$, both in solution (Fig. 2a) and loaded inside the hydrogel, is shown (Fig. 2b). The chonoamperograms (Fig. 2a) show that the signal decays faster in the case of solution than in the hydrogel, suggesting a smaller diffusion coefficient. In both cases, the current gives linear Cottrell plots (Fig. 2b), indicating that the current is diffusion controlled at large enough oxidation potentials. It should be noticed that the signal measured in the hydrogel is larger than in solution.

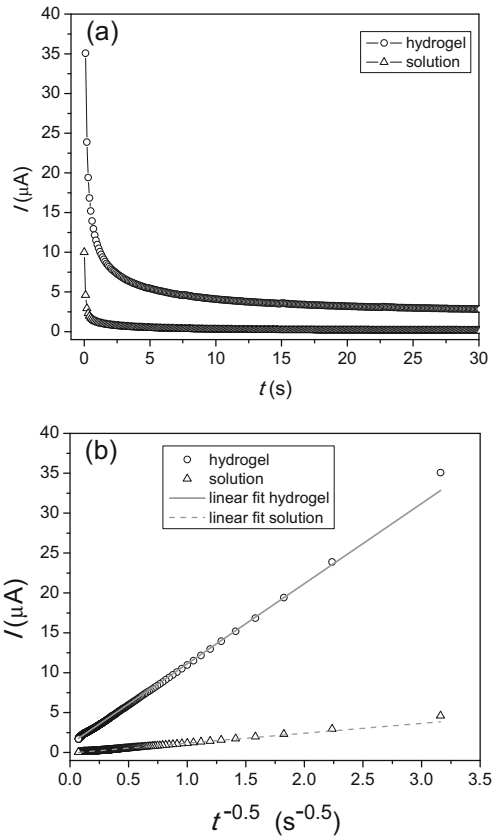

Fig. 2 **a** Chronoamperograms of a GC electrode in a $Fe(phen)_3^{2+}$ solution (0.2 mM in 1 M KCl, *open triangles*) and a GC electrode pressed on a hydrogel (poly(AAm-co-AMPS), *open circles*) loaded with $Fe(phen)_3^{2+}$ (11.4 mM). $A = 0.071\ cm^2$. Potential step from 0.7 to 1.2 V. **b** Cottrell plots calculated from the data shown in **a** . The *open triangles* depict data measured in solution, while the *open triangles* show data measured in the hydrogel

From the slopes of the Cottrell plots, it is possible to calculate the diffusion coefficients in both media, using Cottrell's equation [28]:

$$i_{\mathrm{cot}}(t) = \frac{(z_{Ox} - z_{\mathrm{Red}})\, FAC_{\mathrm{Red}}\sqrt{D_{\mathrm{Red}}}}{\sqrt{\pi t}} \quad (2)$$

where D_{Red} is the diffusion coefficient, C_{Red} the concentration, A the electrode area, F the Faraday constant, and z_{Ox} and z_{Red} are the charges of the reduced ($Fe(phen)_3^{2+}$) and oxidized ($Fe(phen)_3^{3+}$) species, respectively. From the slope of the Cottrell's plot, a value of $D_{\mathrm{Red}} = 4.1 \times 10^{-7}$ cm^2 s^{-1} can be calculated. However, the calculation assumes that there are no migration effects. The derivation of Cottrell's Eq. (2) from Fick's laws assumes that the mass transport of the electroactive species is solely controlled by diffusion, since a large amount of no electroactive and mobile inert electrolyte, usually called supporting electrolyte, is present.

Inside the hydrogel, such a condition could not be fulfilled since the counterions of the $Fe(phen)_3^{2+}$ redox species (likely the $-SO_3^-$ groups) are immobile. It has been shown that Cottrell's equation still holds under conditions of migration and diffusion of redox ions [29, 30], albeit with correction factors related with the charges of the reduced/oxidized species and the counterions. Specifically, the current transient profiles due to the mass transport of redox charged species inside membrane-type polymers, using the complete Nernst-Planck equation, were simulated by Doblhofer [31]. They found that the current Cottrell's equation is fulfilled, but the measured diffusion coefficient (D_{eff}) differs from the one which would be measured in the presence of excess supporting electrolyte (D_{Red}, Eq. 2). The current values ($i_{\mathrm{eff}}(t)$) will be somewhat larger than those predicted by Cottrell's Eq. (2) [31]. Using the correction factor described in [31], it is possible to calculate the ratio $D_{\mathrm{eff}}/D_{\mathrm{Red}}$ as a function of $D_{\mathrm{Red}}/D_{\mathrm{Ox}}$ [31], for $z_{\mathrm{Red}} = 2$ and $z_{\mathrm{Ox}} = 3$. The values of diffusion coefficient for the reactant ($D_{\mathrm{Red}} = Fe^{2+}$) and product (oxidized species ($D_{\mathrm{Ox}} = Fe^{3+}$) inside the hydrogel are not known, but the ratio $D_{\mathrm{Red}}/D_{\mathrm{Ox}}$ is 1.18 in aqueous solution [32] and 1.22 in agarose gel [33]. Using a ratio $D_{\mathrm{Red}}/D_{\mathrm{Ox}} = 1.2$, a correction factor of 0.71 is calculated [31]. Therefore, the effective diffusion coefficient of Fe^{2+} measured inside the hydrogel is of 5.8 (±0.5) × 10^{-7} cm^2 s^{-1}.

Digital simulation of the voltammetric behavior of $Fe(phen)_3^{2+}$ in solution and inside the hydrogel

To ascertain the reaction mechanism, digital simulation of the cyclic voltammetry response was performed. The cyclic voltammogram of $Fe(phen)_3^{2+}$ in solution is simulated using ESP (see exp. part) with a reversible charge transfer, obtaining a good fit (Fig. 3a).

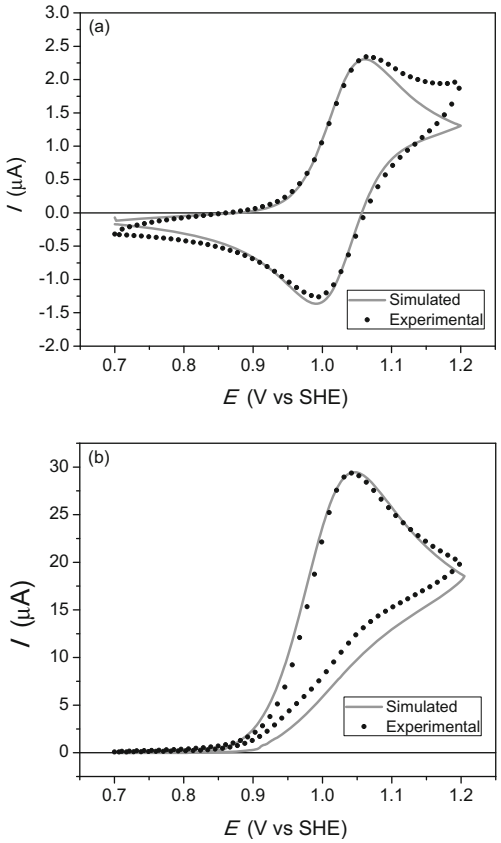

Fig. 3 Digital simulation of the cyclic voltammograms. The experimental data (from Fig. 1) are shown as *black points*, while the simulated data are shown as *gray full lines*. **a** Cyclic voltammogram of $Fe(phen)_3^{2+}$ (0.2 mM) in 1-M KCl solution. Simulation parameters: $E^{\bullet} = 1.066$ V. $ke = 10$ cm s^{-1}. $\alpha = 0.5$. $D_{\text{Red-solution}} = 4.4 \times 10^{-6}$cm^2 s^{-1}. **b** Cyclic voltammogram of $Fe(phen)_3^{2+}$ (11.4 mM) loaded inside a PAAm-co-AMPS hydrogel. Simulation parameters: $E^{\bullet} = 1.066$ V. $ke = 0.5$ cm s^{-1}. $\alpha = 0.5$. $D_{\text{Red-hydrogel}} = 5.7 \times 10^{-8}$cm^2 s^{-1}. $K = 4 \times 10^4$

On the other hand, the voltammogram of $Fe(phen)_3^{2+}$ measured inside the gel (Fig. 1b) has a quite different shape than those measured in solution. The cyclic voltammogram resembles those measured by Ogura and Miyamoto in acetonitrile [24]. The peak oxidation current is significantly larger than the peak reduction current. They proposed a catalytic mechanism involving free iron present in solution:

$$Fe(Phen)_3^{2+} = Fe(Phen)_3^{3+} + e^- \quad \text{(Electrochemical)} \quad (3)$$

$$Fe(Phen)_3^{3+} + Fe^{2+} = Fe(phen)_3^{2+} + Fe^{3+} \quad \text{(Chemical)} \quad (4)$$

The presence of free iron is due to the labile nature of the phenantroline in the complex, which produces the free ion by dissociation of the complex [23]:

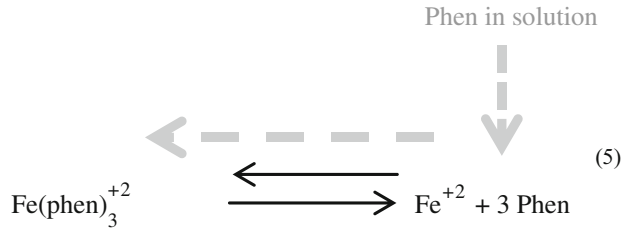

(5)

Since the redox potential of the couple Fe^{2+}/Fe^{3+} (0.771 V vs NHE) is lower than the one for $Fe(phen)_3^{2+}/Fe(phen)_3^{3+}$ (1.066 V vs NHE), the catalytic step is energetically favored. While free Fe^{2+} could be oxidized on the electrode, it is known that the heterogeneous charge transfer constant for Fe^{2+} oxidation on polished glassy carbon is quite small [34]. Therefore, the catalytic pathway occurs at faster rate than the direct electrochemical oxidation.

The digital simulation of the cyclic voltammogram measured inside the hydrogel using an EC mechanism gives a good fit of the experimental data (Fig. 4b). The rate constant for the oxidation of Fe^{2+}(aq) by $Fe(phen)_3^{3+}$ was obtained from reported values in solution [35]. The presence of the hydrogel matrix seems not only to change the mechanism from a reversible (E_{rev}, ke = 10 cm/s) electrochemical single step to an electrochemical-chemical ($E_{qrev}C_{cat}$) reaction but also to decrease the charge transfer constant to a lower value ($ke = 0.5$ cm s^{-1}). Therefore, the loading of the complex inside the hydrogel seems to significantly affect the environment of the chemical reaction.

The presence of a large concentration of anionic groups ($-SO_3^-$) inside the hydrogel could affect both the complexation equilibrium and the mass transport of all species. Fe^{2+} is effectively retained inside the hydrogel with a partition coefficient of ca. 50, quite similar to that of the complex. Therefore, it is likely that the labile complex [23] could produce free iron which is retained inside the hydrogel.

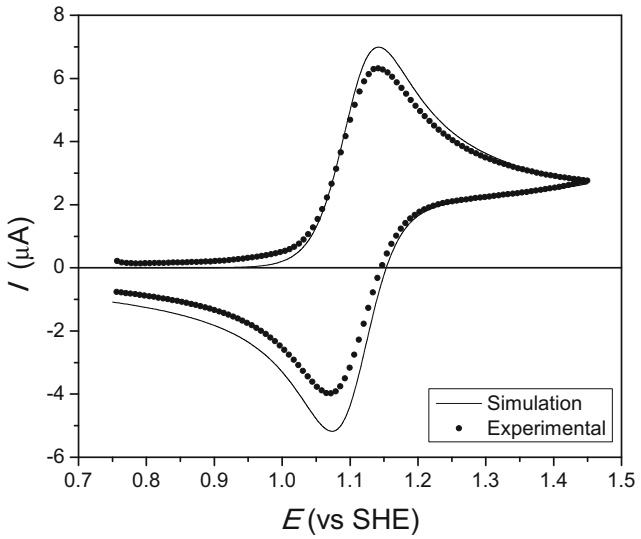

Fig. 4 Electrochemical response of $Fe(phen)_3^{2+}$ (11.4 mM) loaded inside a PAAm-co-AMPS hydrogel in the presence of excess phenanthroline (10 mM) (*black points*). Digital simulation of the CV (*full line*). Simulation parameters: $E^{\bullet}$ = 1.066 V. $ke = 10^4$ cm s^{-1}. $\alpha = 0.5$. $D_{Red} = 5.5 \times 10^{-8}$ cm^2 s^{-1}

Cyclic voltammetry and chronoamperometry in the presence of excess phenanthroline

To test if the $E_{qrev}C_{cat}$ mechanism is due to free iron present, we load the free ligand (Phen) into the hydrogel with the complex, to shift the equilibrium (Eq. 5) toward the formation of the complex. In that way, the free iron concentration inside the hydrogel decreases to negligible levels and the EC mechanism will become a simple electrochemical one (E). The cyclic voltammogram measured with an excess phenanthroline loaded (Fig. 4) shows a single reversible oxidation/reduction likely due to the electrochemistry of the $Fe(phen)_3^{2+}$ complex absorbed inside the hydrogel.

The simulation of the cyclic voltammogram with a single reversible redox step (E_{rev}) seems to fit quite well the measured profile in terms of shape and peak potentials (Fig. 4). Interestingly, the charge transfer constant is larger than in the case of the $E_{qrev}C_{ca}$, making it an E_{rev} instead of a E_{qrev}, analogously to the electrochemistry of $Fe(phen)_3^{2+}$ in solution. Moreover, if the excess phenanthroline is removed and an excess of Fe^{2+} is loaded inside the hydrogel, the cyclic voltammogram (Fig. S2, supporting information) becomes similar to the one depicted in Fig. 1b, restoring the electrochemical-chemical mechanism.

While the fitting is good, the experimental currents are larger than the simulated values. Since the latter are simulated assuming excess supporting electrolyte, the difference could be related to the effect of migration of redox ions on the current. The influence of migration on cyclic voltammograms has been simulated for experiments with large and small amounts of supporting electrolyte by Stevens and Bond [36]. They predict that the Randles-Sevcik equation still holds, but for oxidations, the current values should be smaller than those measured in the presence of excess of non-electroactive supporting electrolyte. The experimental data agree with the prediction, being the currents measured inside the hydrogel, where no excess of supporting electrolyte is present due to ion exclusion, smaller than the simulated ones. Moreover, Stevens and Bond [36] predicted that the difference between current values with supporting electrolyte (simulated in our case) and without supporting electrolyte (measured in our case) should be different for the oxidation than reduction scan. Such a behavior can be qualitatively observed in Fig. 4. The cyclic voltammograms, measured at different scan rates, show currents which increase with the scan rate (Fig. 5a). As predicted by Stevens and Bond [36], Randles-Sevcik equation should hold when migration of the redox species is present, implying

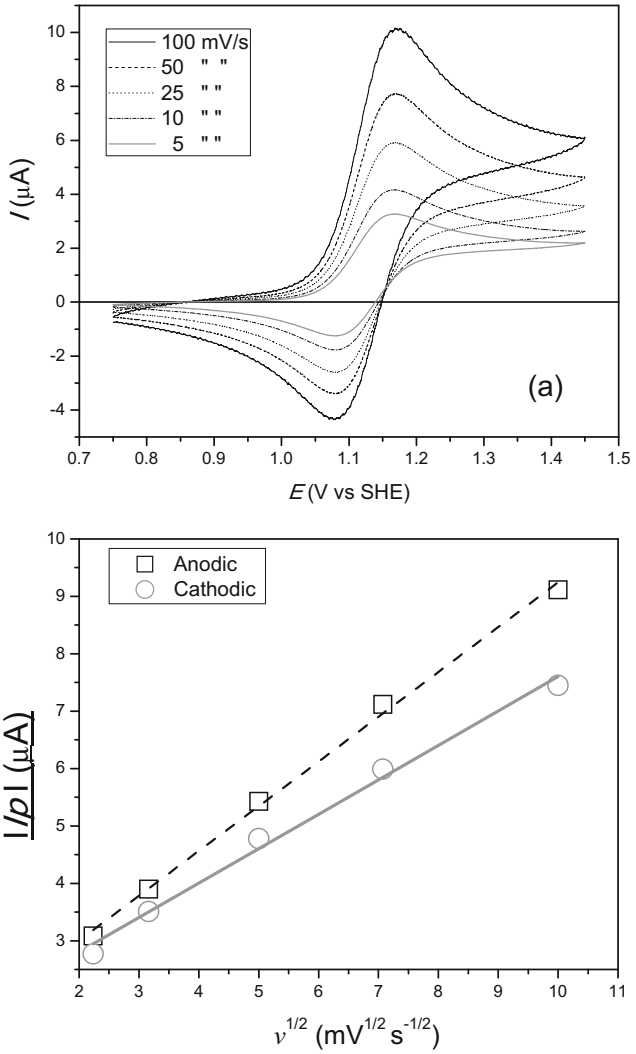

Fig. 5 **a** Cyclic voltammograms of a glassy carbon electrode in 11.4 mM ($Fe(phen)_3^{2+}$) in a PAAm-co-AMPS hydrogel, in the presence of excess (10 mM) phenanthroline, at different scan rates (see *insert*). $A = 0.071$ cm^2, $T = 25$ °C. **b** Randles-Sevcik plot depicting the modulus of the peak current as a function of the square root of the scan rate. Data obtained from **a**

that peak currents should show a linear dependence with the square root of scan rate (Fig. 5b). However, the dependence of the modulus of the peak currents should be different for oxidation and reduction, due to migration effects, while in the presence of a large amount of supporting electrolyte, both slopes should be the same [38]. The linear plots of the dependence of the modulus of the peak current with the square root of the scan rate show a different slope (Fig. 5b).

As expected, the current transient in this system should obey Cottrell's equation [31], giving linear plots of current with the square root of time. Such behavior is experimentally observed (Fig. S1, supplementary information). From the slope, a diffusion coefficient, $D_{Red} = 3.9\ (\pm 0.5) \times 10^{-8}$ cm^2 s^{-1}, is obtained.

As before, the value has to be corrected for migration effects. In this case, it is assumed that the diffusion coefficients for the reactant ($D_{Red} = Fe(phen)_3^{2+}$) and product (oxidized species ($D_{Ox} = Fe(phen)_3^{3+}$) are the same. This is a reasonable assumption, given the large size of the cations which lead to a small difference of charge/area ratio between both species and therefore imply a negligible change in the hydration sphere size [37]. Using a ratio $D_{Red}/D_{Ox} = 1$, the correction factor is 0.76 [31].

Therefore, the corrected diffusion coefficient of $Fe(phen)_3^{2+}$ inside the hydrogel is of $D_{Red\text{-}hydrogel} = 5.5\ (\pm 0.5) \times 10^{-8}$ cm^2 s^{-1}. This value is ca. 80 times smaller than the one measured in solution ($D_{Red\text{-}solution} = 4.4\ (\pm 0.5) \times 10^{-6}$ cm^2 s^{-1}). The latter value is close to that measured by Bard and coworkers by cyclic voltammetry ($D_{Red\text{-}solution} = 4.9\ (\pm 0.5) \times 10^{-6}$ cm^2 s^{-1} [25]. Therefore, a clear matrix effect is observed involving the slower mass transport of redox couples inside the hydrogel.

Buttry and Anson [18] review the values measured for different redox couples inside the same polyelectrolyte (Nafion®) film and reported values as low as $D = 1 \times 10^{-12}$ cm^2 s^{-1} (for $Co(bpy)_3^{2+}$) and as high as $D = 2 \times 10^{-9}$ cm^2 s^{-1} for $Ru(NH_3)_3^{2+}$ The value reported here for $Fe(phen)_3^{2+}$ loaded inside a hydrogel is somewhat larger, but it should be taken into account that the hydrogel structure is more open than a typical Nafion® film. On the other hand, diffusion coefficients of smaller molecules (phenol) in poly(*N*-isopropylacrylamide) films have been measured to be $D = 7.4 \times 10^{-8}$ cm^2 s^{-1} (at 25 °C and 0.01 mM) [38]. The diffusion coefficient of the much larger bovine serum albumin is 4.9×10^{-8} cm^2 s^{-1} (at 25 °C and 0.01 M). Recently, Leddy and coworkers measured the diffusion coefficient of $Ru(bpy)_3^{2+}$ in Nafion® to be $D = 2.4\ (\pm 0.07) \times 10^{-8}$ cm^2/s [39].

Therefore, the measured value for $Fe(phen)_3^{2+}$, of intermediate size, is reasonable. It is noteworthy that the measured diffusion coefficient is quite close to that reported for electropolymerized Tris[5-amino-1,10-phenanthroline]iron(II) ($D = 3.10\ (\pm 0.09) \times 10^{-8}$ cm^2 s^{-1}), which contains the same redox moiety [14]. However, in the latter case, the apparent diffusion coefficient is controlled by electron hoping or counterion diffusion since the redox species are immobile.

The viscoelastic properties of the hydrogel depend on parameters of the material like the swelling ratio, the degree of crosslinking, the mechanical pressure, and the polymerization kinetics [40]. It has been shown that the diffusion coefficient of $Fe(phen)_3^{2+}$, in aqueous solutions of inert salts, obeys Stokes's law [32]. That is, the product of the diffusion coefficient and the viscosity ($D\eta$) is a constant unless specific interactions are present. As it has been previously reviewed [41], solute diffusion inside hydrogels is a complex process and different models have been used to account for phenomena like dependence on the concentration of the solute and/or the effect on the viscoelastic properties of the hydrogels.

Therefore, the measurement of the diffusion coefficient of $Fe(phen)_3^{2+}$ inside the hydrogel, using chronoamperometry, could be used to probe the viscoelastic properties of the hydrogels and/or to shed light into the mechanism of mass transport.

In all calculations, it is assumed that the electrochemical active area corresponds to the geometrical area of the electrode. This is the usual assumption when diffusion coefficients are measured in electrodes covered by layers of redox hydrogels [13, 14] and seems to be valid in our case. It could be envisaged that hydrophobic and hydrophilic domains exist, but both acrylamide [42] and AMPS are highly hydrophilic monomer units [43]. Moreover, this approach is also applied to Nafion® where it is known that hydrophobic domains exist [44].

One remaining question is the nature of the measured diffusion coefficient. The metal complex can physically diffuse along the hydrogel (Fig. S3, supporting information) driven by a concentration gradient. Therefore, the measured coefficient is likely due to physical transport of $Fe(phen)_3^{2+}$ and not necessarily to electron hoping between oxidized and reduced metal complexes electrostatically bound. The relatively low concentration of redox complex inside the hydrogel (11.4 mM) makes the electron hoping difficult due to the relatively large distance between redox centers. In fact, it is significantly smaller than the values measured in Nafion® (159 mM [44]), where electron hoping between redox centers is the accepted mechanism of electron transport. The physical mass transport of $Fe(phen)_3^{2+}$ is likely to be affected by the presence of anionic groups in the matrix. Electrochemical measurements of $Fe(phen)_3^{2+}$ loaded inside neutral and cationic hydrogels could help to ascertain the role of columbic interactions on mass transport.

Conclusions

A simple setup allows to perform electrochemistry of a redox couple ($Fe(phen)_3^{+2}$) inside a hydrogel matrix and compare with the behavior of the same couple in solution. The electrochemical properties of the redox couple are strongly affected by the presence of the hydrogel matrix. The redox mechanism seems to change from a quasi-reversible electrochemical mechanism to electrochemical-chemical mechanism, probably linked to a catalytic reaction with free Fe^{+2} ions present inside the hydrogel. Digital simulation of the cyclic voltammograms, using an electrochemical (quasi-reversible)-chemical (catalytic) ($E_{qrev}C_{cat}$) mechanism, allows to fit the observed response. The heterogeneous charge transfer constant for $Fe(phen)_3^{2+}$ oxidation seems to decrease from the value measured in solution. Moreover, addition of free ligand (phenanthroline) shifts the complexation equilibrium toward the redox complex formation effectively changing the mechanism from an electrochemical-chemical ($E_{qrev}C_{cat}$) oxidation of free iron catalyzed by the redox complex into a simple electrochemical (E_{rev}) oxidation of the complex. The presence of a $E_{qrev}C_{cat}$ mechanism suggests the use of the hydrogel loaded with $Fe(phen)_3^{2+}$ as an electrochemically driven redox catalyst in electroanalytical chemistry, as it has been done with similar redox complexes adsorbed in clays [45] or polyelectrolytes [46]. One advantage over thin film-modified electrodes would be the fact that the analyte (e.g., tryptophan [4]) could also be partitioned to give a higher concentration inside the hydrogel, therefore increasing the overall current. Another is that the analyte could be loaded inside the hydrogel from complex matrixes, removed, washed, and the electrochemistry performed in clean electrolytes. Such two-step preconcentration and measuring method resembles solid-phase extraction and could not be performed with soluble redox catalysts or immobilized thin films, which have to be used in situ. Moreover, a thick piece of hydrogel loaded with a redox couple has a true semi-infinite boundary condition in any experimentally accessible time frame (e.g., at slow scan rate in cyclic voltammetry), similar to a large electrochemical cell filled with solution. Therefore, there is no accessible hydrogel/solution boundary, only an electrode/hydrogel boundary. As it has been shown recently by Leddy and coworkers, it is not the case for film-modified electrodes (even for thicknesses of several μm) where special diagnostic criteria have been proposed to ascertain the nature of the mass transport regime in each time frame [39].

The chronoamperometric transients fit Cottrells' plot but with a corrected diffusion coefficient, which takes into account the effect of migration, following the simulation of Lange and Doblhofer [31]. The diffusion coefficient of $Fe(phen)_3^{2+}$ ($D_{Red\text{-}hydrogel} = 5.5\ (\pm 0.5) \times 10^{-8}\ cm^2\ s^{-1}$) measured inside the hydrogel is ca. 80 times smaller than the one measured in solution ($D_{Red\text{-}solution} = 4.4\ (\pm 0.5) \times 10^{-6}\ cm^2\ s^{-1}$). The cyclic voltammogram measured in the presence of excess ligand could be simulated with a simple electrochemical (E_{rev}) mechanism, but some differences are observed in the current values due to migration effects [38]. Moreover, the voltammogram's peak currents could be fitted with Randles-Sevcik equation, which means that they are linear with the square root of the scan rate. However, the slope is different for the oxidation than reduction, as predicted by the simulation considering migration effects [38].

The simple experimental setup allows probing hydrogels having different chemical structures, different porosities, and/or the effect of external parameters (pH, temperature, ionic force, etc.) on the physicochemical properties of the hydrogel matrix. It is noteworthy that the physicochemical properties of the hydrogel matrix can be extensively characterized independently, while that is not usually the case of polymer films deposited on electrodes. Additionally, it is quite easy to load

chemical substances inside the hydrogels [4]. Therefore, it is possible to study the effect of the hydrogel matrix on the electrochemical properties of different absorbed substances by comparison with the response in solution. While this is also the case for substances absorbed into films of polymers deposited onto electrodes, it is not the case for hydrogels with covalent linked groups whose synthesis and characterization are quite complex. Therefore, a wider diversity of hydrogels and redox probes can be tested toward a better understanding and more useful applications. Additional studies are being performed along these research lines in our laboratory.

Acknowledgments D.F. Acevedo, C.R. Rivarola, M.M. Bruno, and C.A. Barbero are permanent research fellows of CONICET. M.V. Martinez and R. Coneo Rodriguez thank CONICET for graduate fellowships. The funding of CONICET and SPU is gratefully acknowledged. Prof. Carlo Nervi is gratefully acknowledged for the use of ESP 2.0. Helpful suggestions by the reviewers are gratefully acknowledged.

References

1. Kalia S (2016) Polymeric hydrogels as smart biomaterials. Springer, Berlin
2. Loh JX, Scherman OA (2013) Polymeric and self assembled hydrogels, from fundamental understanding to applications. The Royal Society of Chemistry, Cambridge
3. Dunn MJ (ed) (1986) Gel electrophoresis of proteins. IOP, Bristol
4. Molina M, Rivarola C, Barbero C (2012) Study on partition and release of molecules in superabsorbent thermosensitive nanocomposites. Polymer 53:445–453
5. Simpson NJK (2000) Solid-phase extraction, principles, techniques, and applications. Marcel Dekker, Basel
6. Bagel O, Degrand C, Limoges B (1999) Ion-exchange voltammetry as a solid-phase Microextraction analytical method: factors influencing the mass transfer to Perfluorosulfonated ionomer film-coated electrodes and some of their consequences on the current responses. Anal Chem 71:3192–3199
7. Aguilar M, Cortina JL (eds) (2008) Solvent extraction and liquid membranes: fundamentals and applications in new materials. CRC Press, Boca Raton
8. Lyons M (ed) (1996) Electroactive polymer electrochemistry part 2: methods and applications. Springer, Berlin
9. Grumelli DE, Wolosiuk A, Forzani E, Planes G, Barbero C, Calvo EJ (2003) Probe beam deflection study of ion exchange in self-assembled redox polyelectrolyte thin films. Chem Commun 3014–3015
10. Andrieux CP, Haas O, Saveant JM (1986) Catalysis of electrochemical reactions at redox-polymer-coated electrodes. Mediation of the iron(III)/iron(II) oxido-reduction by a polyvinylpyridine polymer containing coordinatively attached bisbipyridine chlororuthenium redox centers. J Am Chem Soc 108:8175–8182
11. Ju H, Leech D (1997) Electrochemistry of poly(vinylferrocene) formed by direct electrochemical reduction at a glassy carbon electrode. J Chem Soc Faraday Trans 93:1371–1375
12. Inzelt G, Szabo L (1986) The effect of the nature and the concentration of counter ions on the electrochemistry of poly(vinylferrocene) polymer film electrodes. Electrochim Acta 31:381–1387
13. Forster RJ, Vos JG, Lyons MEG (1991) Controlling processes in the rate of charge transport through $[Os(bipy)_2(PVP)_nCl]Cl$ redox polymer-modified electrodes. J Chem Soc Faraday Trans 87: 3761–3767
14. Nyasulu FWM, Mottola HA (1988) Electrochemical behavior of 5-amino-1,10-phenanthroline and oxidative electropolymerization of tris[5-amino-1,10-phenanthroline]iron(II). J Electroanal Chem Interfacial Electrochem 239:175–186
15. Bachas LG, Cullen L, Hutchins RS, Scott DL (1997) Synthesis, characterization and electrochemical polymerization of eight transition-metal complexes of 5-amino-l,10-phenanthroline. J Chem Soc Dalton Trans 9:1571–1577
16. Barbero C, Miras MC, Calvo EJ, Kötz R, Haas O (2002) A probe beam deflection study of ion exchange at poly(vinylferrocene) films in aqueous and nonaqueous electrolytes. Langmuir 18:2756–2764
17. Rubinstein I (1986) Structural effects on the electrochemistry of ferrocene in Nafion films on electrodes. J Electroanal Chem 200: 405–410
18. Buttry DA, Anson FC (1983) Effects of electron exchange and single-file diffusion on charge propagation in Nafion films containing redox couples. J Am Chem Soc 105:685–689
19. Buriez O, Moretto LM, Ugo P (2006) Ion-exchange voltammetry of tris(2,2isbipyridine) nickel(II), cobalt(II), and Co(salen) at polyestersulfonated ionomer coated electrodes in acetonitrile: reactivity of the electrogenerated low-valent complexes. Electrochim Acta 52:958–964
20. Silambarasan K, Kumar AVN, Joseph J (2016) K4[Fe(CN)6] immobilized anion sensitive protonated amine functionalized polysilsesquioxane films for ultra-low electrochemical detection of dsDNA. Phys Chem Chem Phys 18:7468–7474
21. Oh SM, Faulkner LR (1989) Electron transport dynamics in partially quaternized poly(4-vinylpyridine) thin films containing ferri/ferrocyanide. J Electroanal Chem 269:77–97
22. AA S, Belcher R, Freiser H (1969) Analytical applications of 1,10-phenanthroline and related compounds volume 32. International Series of Monographs on Analytical Chemistry Elsevier, Amsterdam
23. Luque de Castro MD, Valcarcel M, Albahadyl FN, Mottola HA (1987) Electrochemical behaviour of iron-1,10-phenanthroline complexes at a carbon paste electrode. J. Electroanal Chem 219: 139–151
24. Ogura K, Miyamoto K (1978) Electrode reaction of tris(1-10-phenanthroline)iron(I) complex in aqueous and nonaqueous solvents. Electrochim Acta 23:509–512
25. Carter MT, Rodriguez M, Bard AJ (1989) Voltammetric studies of the interaction of metal chelates with DNA. 2. Tris-chelated complexes of cobalt(III) and iron(II) with 1,10-phenanthroline and 2,2′-bipyridine. J Am Chem Soc 111:8901–8911
26. Vallejos S, Munoz A, Ibeas S, Serna F, Garcia FC, Garcia JM (2013) Solid sensory polymer substrates for the quantification of iron in blood, wine and water by a scalable RGB technique. J Mater Chem A 1:15435–15441
27. http://lem.ch.unito.it/chemistry/esp_manual.html (accessed 1/02/2016).
28. Bard AJ, Faulkner LR (1980) Electrochemical methods: fundamentals and applications. Wiley, New York
29. Myland JC, Oldham KB (1999) Limiting currents in potentiostatic voltammetry without supporting electrolyte. Electrochem Commun 1:467–471
30. Bieniasz LK (2002) Analytical formulae for chronoamperometry of a charge neutralisation process under conditions of linear migration and diffusion. Electrochem Commun 4:917–921
31. Lange R, Doblhofer K (1987) The transient response of electrodes coated with membrane/type polymer films under conditions of diffusion and migration of the redox ions. J Electroanal Chem 237:13–26
32. Spiro M, Creeth AM (1990) Tracer diffusion coefficients of I-, I3-, Fe2+, Fe3+ at low temperatures. J Chem Soc Faraday Trans 86: 3573–3576

33. Balcom BJ, Leest TJ, Sharp AR, Kulkamis NS, Wagner GS (1995) Diffusion in Fe(II/III) radiation dosimetry gels measured by magnetic resonance imaging. Phys Med Biol 40:1665–1676
34. Barbero C, Silber JJ, Sereno L (1988) Studies of surface-modified glassy carbon electrodes obtained by electrochemical treatment. Its effect on $Ru(bpy)_3^{2+}$ adsorption and the electron transfer rates of the Fe2+/Fe3+ couple. J Electroanal Chem 248:321–340
35. Sutin B, Gordon BM (1961) The kinetics of the oxidation of the iron (II) ion by the tris(1,10-phenanthroline)-iron(II) J. Am Chem Soc 83:70–73
36. Stevens NPC, Bond AM (2002) The influence of migration on cyclic and rotating disk voltammograms. J Electroanal Chem 538-539:25–33
37. Tominaga T, Matsumoto S, Koshiba T, Yamamoto Y (1988) Tracer diffusion of the tris(1,10-phenanthroline)iron(II) Cation in aqueous salt solutions. Effect of hydrophobic interactions. J Chem Soc Faraday Trans I 84:4261–4266
38. Naddaf AA, Bart H-J (2011) Diffusion coefficients in thermosensitive poly(NIPAAm) hydrogels. Macromol Symp 306-307:150–165
39. Knoche KL, Hettige C, Moberg PD, Amarasinghe S, Leddy J (2013) Cyclic voltammetric diagnostics for inert, uniform density films. J Electrochem Soc 160:H285–H293
40. Rivero RE, Alustiza F, Rodríguez N, Bosch P, Miras MC, Rivarola CR, Barbero CA (2015) Effect of functional groups on physicochemical and mechanical behavior of biocompatible macroporous hydrogels. React Funct Polym 97:77–85
41. Amsden B (1998) Solute diffusion within hydrogels. Mech Models Macromol 31:8382–8395
42. Aliev R (2001) Hydrophilicity and surface energy of polyethylene modified by radiation grafting of acrylamide. Polym Bull 47:99–104
43. Matsukata M, Hirata M, Gong JP, Osada Y, Sakurai Y, Okano T (1998) Two-step surfactant binding of solvated and cross-linked poly(*N*-isopropylacrylamide-co- (2-acrylamido-2-methyl propane sulfonic acid)). Colloid Polym Sci 276:11–18
44. Gellett WL, Knoche KL, Rathuwadu NPW, Leddy J (2016) Electron hopping of tris (2,2′ bipyridyl) transition metal complexes $M(bpy)_3^{2/3}$ in Nafion. J Electrochem Soc 163:H588–H597
45. Azad UA, Turllapati S, Rastogi PK, Ganesan V (2014) Tris(1,10-phenanthroline)iron(II)-bentonite film as efficient electrochemical sensing platform for nitrite determination. Electrochim Acta 127:193–199
46. Azad UP, Ganesan V (2010) Efficient sensing of nitrite by $Fe(bpy)_3^{2+}$ immobilized Nafion modified electrodes. Chem Commun 46:6156–6158